Constraints on models for the initial collision geometry
in ultra relativistic heavy ion collisions

Roy A. Lacey,[1, 2, *] Rui Wei,[1] N. N. Ajitanand,[1] J. M. Alexander,[1] X. Gong,[1] J. Jia,[1, 2] A. Taranenko,[1]
R. Pak,[2] and Horst Stöcker[3]

[1]*Department of Chemistry, Stony Brook University,*
Stony Brook, NY, 11794-3400, USA
[2]*Physics Department, Brookhaven National Laboratory,*
Upton, New York 11973-5000, USA
[3]*Institut für Theoretische Physik, Johann Wolfgang Goethe-Universität*
D60438 Frankfurt am Main, Germany
(Dated: October 30, 2018)

Monte Carlo simulations are used to compute the centrality dependence of the collision zone eccentricities ($\varepsilon_{2,4}$), for both spherical and deformed ground state nuclei, for different model scenarios. Sizable model dependent differences are observed. They indicate that measurements of the 2nd and 4th order Fourier flow coefficients $v_{2,4}$, expressed as the ratio $\frac{v_4}{(v_2)^2}$, can provide robust constraints for distinguishing between different theoretical models for the initial-state eccentricity. Such constraints could remove one of the largest impediments to a more precise determination of the specific viscosity from precision $v_{2,4}$ measurements at the Relativistic Heavy Ion Collider (RHIC).

Energetic collisions between heavy ions at the Relativistic Heavy Ion Collider (RHIC), produce a strongly interacting quark gluon plasma (QGP). In non-central collisions, the hydrodynamic-like expansion of this plasma [1–6] results in the anisotropic flow of particles in the plane transverse to the beam direction [7, 8]. At mid-rapidity, the magnitude of this momentum anisotropy is characterized by the even order Fourier coefficients;

$$v_{\mathrm{n}} = \left\langle e^{in(\phi_p - \Phi_{RP})} \right\rangle, \; n = 2, 4, .., \qquad (1)$$

where ϕ_p is the azimuthal angle of an emitted particle, Φ_{RP} is the azimuth of the reaction plane and the brackets denote averaging over particles and events. The elliptic flow coefficient v_2 is observed to dominate over the higher order coefficients in Au+Au collisions at RHIC (*i.e.* $v_n \propto (v_2)^{\frac{n}{2}}$ and $v_2 << 1$) [9, 10].

The magnitudes and trends of $v_{2,4}$ are known to be sensitive to the transport properties of the expanding partonic matter [3, 4, 6, 11–17]. Consequently, there is considerable current interest in their use for quantitative extraction of the specific shear viscosity, *i.e.* the ratio of shear viscosity η to entropy density s of the plasma. Such extractions are currently being pursued via comparisons to viscous relativistic hydrodynamic simulations [16–18], transport model calculations [14, 15] and hybrid approaches which involve the parametrization of scaling violations to ideal hydrodynamic behavior [10, 12, 13]. In all cases, accurate knowledge of the initial eccentricity $\varepsilon_{2,4}$ of the collision zone, is a crucial unresolved prerequisite for quantitative extraction of $\frac{\eta}{s}$.

To date, no direct experimental measurements of $\varepsilon_{2,4}$ have been reported. Thus, the necessary theoretical estimates have been obtained by way of the overlap geometry corresponding to the impact parameter b of the collision, or the number of participants N_{part} in the collision zone. A robust constraint for N_{part} values can be obtained via measurements of the final hadron multiplicity or transverse energy. However, for a given value of N_{part}, the theoretical models used to estimate ε_2 give results which differ by as much as $\sim 25\%$ [19, 20] – a difference which leads to an approximate factor of two uncertainty in the extracted η/s value [16]. Therefore, an experimental constraint which facilitates a clear choice between the different theoretical models is essential for further progress toward precise extraction of η/s.

In ideal fluid dynamics, anisotropic flow is directly proportional to the initial eccentricity of the collision zone. A constant ratio for the flow coefficients $\frac{v_4}{(v_2)^2} \approx 0.5$ is also predicted [21]. It is well established that initial eccentricity fluctuations also influence the magnitude of $v_{2,4}$ significantly [5, 10, 21–23], *i.e.* the presence of these fluctuations serve to increase the value of $v_{2,4}$. Therefore, one avenue to search for new experimental constraints, is to use $\varepsilon_{2,4}$ as a proxy for $v_{2,4}$ and study the model dependencies of their magnitudes and trends vs. N_{part}.

In this communication we present calculated results of $\varepsilon_{2,4}$ for collisions of near-spherical and deformed isotopes, for the Glauber [22, 24] and the factorized Kharzeev-Levin-Nardi (fKLN) [25, 26] models, *i.e.* the two primary models currently employed for eccentricity estimates. We find sizable differences, both in magnitude and trend, for the the ratios $\frac{\varepsilon_4}{(\varepsilon_2)^2}$ obtained from both models. This suggests that systematic comparisons of the measurements for the N_{part} dependence of the ratio $\frac{v_4}{(v_2)^2}$ for these iso-
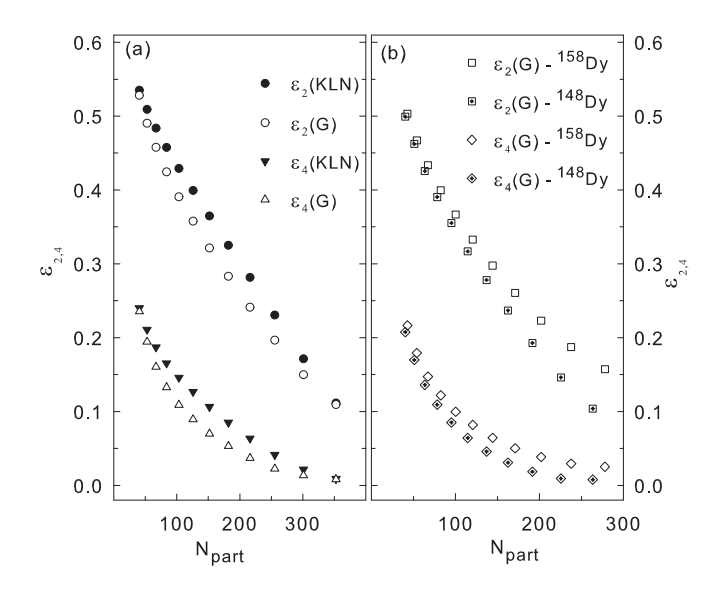
FIG. 1. Calculated values of $\varepsilon_{2,4}$ vs. N_{part} for MC-Glauber (open symbols) and MC-KLN (closed symbols) for Au+Au collisions (a) and near-spherical ^{148}Dy and deformed ^{158}Dy as indicated in (b).

topic systems, can give direct experimental constraints for these models.

Monte Carlo (MC) simulations were used to calculate event averaged eccentricities (denoted here as $\varepsilon_{2,4}$) within the framework of the Glauber (MC-Glauber) and fKLN (MC-KLN) models, for near-spherical and deformed nuclei which belong to an isobaric or isotopic series. Here, the essential point is that, for such series, a broad range of ground state deformations have been observed for relatively small changes in the the number of protons or neutrons [27, 28]. For each event, the spatial distribution of nucleons in the colliding nuclei were generated according to the deformed Woods-Saxon function:

$$\rho(\mathbf{r}) = \frac{\rho_0}{1 + e^{(\mathrm{r} - R_0(1 + \beta_2 Y_{20}(\theta) + \beta_4 Y_{40}(\theta)))/d}}, \quad (2)$$

where R_0 and d are the radius and diffuseness parameters and $\beta_{2,4}$ are the deformation parameters which characterizes the density distribution of the nucleus about its polarization axis (z').

To generate collisions for a given centrality selection, the orientation of the polarization axis for each nucleus (θ_1, ϕ_1 and θ_2, ϕ_2 respectively) was randomly chosen in the coordinate frame whose z axis is the beam direction. For each collision, the values for N_{part} and the number of binary collisions N_{coll} were determined within the Glauber ansatz [24]. The associated $\varepsilon_{2,4}$ values were then evaluated from the two-dimensional profile of the density of sources in the transverse plane $\rho_s(\mathbf{r}_\perp)$, using modified versions of MC-Glauber [24] and MC-KLN [26] respectively.

For each event, we compute an event shape vector S_n and the azimuth of the the rotation angle Ψ_n^* for n-th harmonic of the shape profile [29];

$$S_{nx} \equiv S_n \cos\left(n\Psi_n^*\right) = \int d\mathbf{r}_\perp \rho_s(\mathbf{r}_\perp)\omega(\mathbf{r}_\perp)\cos(n\phi), (3)$$

$$S_{ny} \equiv S_n \sin\left(n\Psi_n^*\right) = \int d\mathbf{r}_\perp \rho_s(\mathbf{r}_\perp)\omega(\mathbf{r}_\perp)\sin(n\phi), (4)$$

$$\Psi_n^* = \frac{1}{n}\tan^{-1}\left(\frac{S_{ny}}{S_{nx}}\right), \quad (5)$$

where ϕ is the azimuthal angle of each source and the weight $\omega(\mathbf{r}_\perp) = \mathbf{r}_\perp{}^2$. The eccentricities were calculated as:

$$\varepsilon_2 = \langle\cos 2(\phi - \Psi_2^*)\rangle \quad \varepsilon_4 = \langle\cos 4(\phi - \Psi_2^*)\rangle \quad (6)$$

where the brackets denote averaging over sources, as well as events belonging to a particular centrality or impact parameter range. For the MC-Glauber calculations, an additional entropy density weight was applied reflecting the combination of spatial coordinates of participating nucleons and binary collisions [19, 23] ;

$$\rho_s(\mathbf{r}_\perp) \propto \left[\frac{(1-\alpha)}{2}\frac{dN_{\text{part}}}{d^2\mathbf{r}_\perp} + \alpha\frac{dN_{\text{coll}}}{d^2\mathbf{r}_\perp}\right], \quad (7)$$

where $\alpha = 0.14$ was constrained by multiplicity measurements as a function of N_{part} for Au+Au collisions [30].

The procedures outlined above (cf. Eqs. 2 - 7) ensure that, in addition to the fluctuations which stem from the orientation of the initial "almond-shaped" collision zone [relative to the impact parameter], the shape-induced fluctuations due to nuclear deformation are also taken into account. Note that $\varepsilon_{2,4}$ (cf. Eq. 6) correspond to $v_{2,4}$ measurements in the so-called participant plane [22, 24]. That is, the higher harmonic ε_4 is evaluated relative to the principal axis determined by maximizing the quadrupole moment. This is analogous to the measurement of v_4 with respect to the 2$^{\text{nd}}$ order event-plane in actual experiments. One consequence is that the density profile is suppressed, as well as the moment for the higher harmonic.

Calculations were performed for a variety of isotopes and isobars with a broad range of known $\beta_{2,4}$ values. Here, we show and discuss only a representative set of results for ^{197}Au ($R = 6.38\,\text{fm}$, $\beta_2 = -0.13$, $\beta_4 = -0.03$), ^{148}Dy ($R = 5.80\,\text{fm}$, $\beta_2 = 0.00$, $\beta_4 = 0.00$) and ^{158}Dy ($R = 5.93\,\text{fm}$, $\beta_2 = 0.26$, $\beta_4 = 0.06$) [27, 28]. For these calculations we used the value $d = 0.53\,\text{fm}$.

Figure 1(a) shows a comparison of $\varepsilon_{2,4}$ vs. N_{part} for MC-Glauber (open symbols) and MC-KLN (filled symbols) for Au+Au collisions. The filled symbols indicate larger $\varepsilon_{2,4}$ values for MC-KLN over most of the considered N_{part} range. The effect of shape deformation is illustrated in Fig. 1(b) where a comparison of $\varepsilon_{2,4}$ vs. N_{part} [for MC-Glauber] is shown for the two Dy isotopes indicated. Both ε_2 and ε_4 show a sizable increase for the isotope with the largest ground state deformation
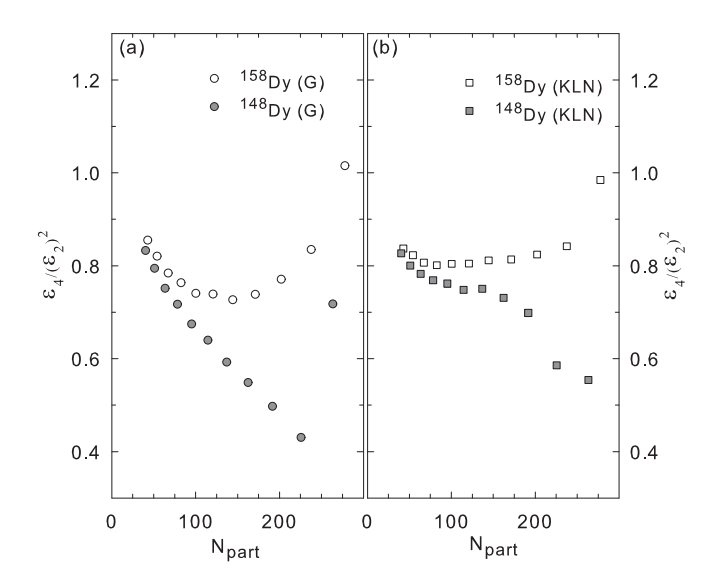
FIG. 2. Comparison of $\frac{\varepsilon_4}{(\varepsilon_2)^2}$ vs. N_{part} for near-spherical ^{148}Dy (filled symbols) and deformed ^{158}Dy (open symbols) collisions. Results are shown for MC-Glauber (a) and MC-KLN (b) respectively.

FIG. 3. N_{part} dependence of $\frac{\varepsilon_4}{(\varepsilon_2)^2}$ (a), $\frac{\varepsilon_4(m)}{(\varepsilon_2(m))^2}$ (b) and $\frac{\text{R}(m)}{(\text{R})}$ (c) for Au+Au collisions (see text). The open and closed symbols indicate the results from MC-Glauber and MC-KLN respectively.

(^{158}Dy). This reflects the important influence of shape-driven eccentricity fluctuations in collisions of deformed nuclei [31–34]. The magnitudes and trends of all of these eccentricities are expected to influence the measured values of $v_{2,4}$ for these systems.

A priori, the model-driven and shape-driven eccentricity differences shown in Fig. 1, need not be the same for ε_2 and ε_4. Therefore, we present the ratio $\frac{\varepsilon_4}{(\varepsilon_2)^2}$ vs. N_{part}, for both models in Fig. 2. The ratios obtained for ^{148}Dy (near-spherical) and ^{158}Dy (deformed) with MC-Glauber are compared in Fig. 2(a); the same comparison is given in Fig. 2(b) but for MC-KLN calculations. Fig. 2(a) indicates a significant difference between the ratio $\frac{\varepsilon_4}{(\varepsilon_2)^2}$ for ^{148}Dy and ^{158}Dy over the full range of N_{part} considered. This difference stems from additional shape-driven fluctuations present in in collisions of ^{158}Dy, but absent in collisions of ^{148}Dy. The same comparison for MC-KLN results, shown in Fig. 2(b), points to a smaller difference for these ratios, as well as a different N_{part} dependence. We attribute this to the difference in the transverse density distributions employed in MC-Glauber and MC-KLN.

For a given value of N_{part}, the measured ratio of the flow coefficients $\frac{v_4}{(v_2)^2}$ for ^{158}Dy+^{158}Dy and ^{148}Dy+^{148}Dy collisions, are expected to reflect the magnitude and trend of the ratio $\frac{\varepsilon_4}{(\varepsilon_2)^2}$ (note that a constant ratio ≈ 0.5 is predicted for ideal hydrodynamics without the influence of fluctuations [21]). Fig. 2 suggests that a relatively clear distinction between fKLN-like and Glauber-like initial collision geometries could be made via systematic studies of $\frac{v_4}{(v_2)^2}$ for near-spherical and deformed isotopes/isobars. Specifically, a relatively smaller (larger)
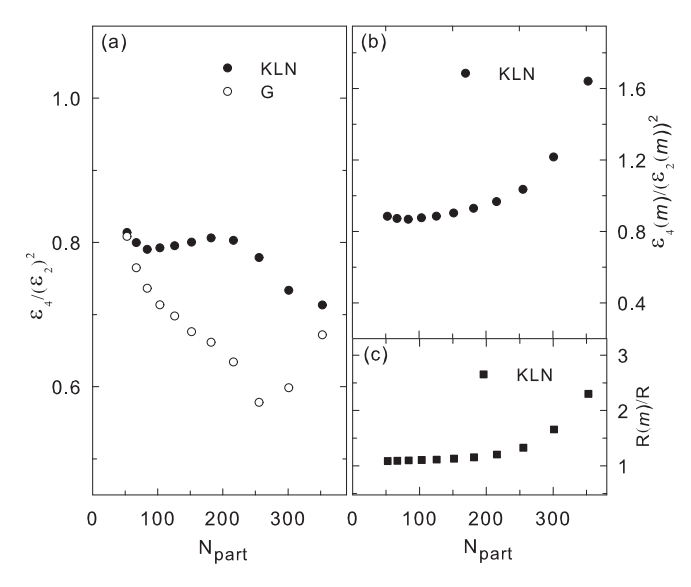
difference between the ratios $\frac{v_4}{(v_2)^2}$ for each isotope, would be expected for fKLN (Glauber) initial geometries. Similarly the scaling of $v_{2,4}$ data from the isotopic or isobaric pair would be expected only for MC-Glauber or MC-KLN eccentricities. Note that the influence of a finite viscosity is expected to be the same for both systems and therefore would not change these conclusions.

The filled symbols in Figs. 2 (a) and (b) also suggest a substantial difference in the $\frac{\varepsilon_4}{(\varepsilon_2)^2}$ ratios predicted by MC-Glauber and MC-KLN respectively, for collisions between near-spherical nuclei. This difference is also apparent in Fig. 3(a) where the calculated ratios for Au+Au ($\beta_2 = -0.13$, $\beta_4 = -0.03$) collisions are shown. The MC-KLN results (filled circles) indicate a relatively flat dependence for $40 \lesssim N_{\text{part}} \lesssim 200$, which contrasts with the characteristic decrease, for the same N_{part} range, seen in the MC-Glauber results.

As discussed earlier, each of these trends is expected to influence the measured ratios of the flow coefficients $\frac{v_4}{(v_2)^2}$. Therefore, an experimental observation of a relatively flat N_{part} dependence for $\frac{v_4}{(v_2)^2}$ [over the range $40 \lesssim N_{\text{part}} \lesssim 200$], could be an indication for fKLN-like collision geometries in Au+Au collisions. Such a trend has been observed in the preliminary and final data sets reported in Refs. [10, 21, 35] and is consistent with the conclusions reached in Ref. [10, 36] that the N_{part} and impact parameter dependence of the eccentricity scaled flow coefficients $\frac{v_2}{\varepsilon_2}$ and $\frac{v_4}{\varepsilon_4}$ favor fKLN-like initial collision geometries.

The closed symbols in Figs. 2(b) and 3(a) indicate a decreasing trend for $\frac{\varepsilon_4}{(\varepsilon_2)^2}$ for near-spherical nuclei for

$N_{\text{part}} \gtrsim 200$. This decrease can be attributed to the fact that, in each event, ε_4 is computed in the reference frame which maximizes the quadrupole shape distribution, *i.e.* the so-called *participant* frame. In this frame, ε_4 can take on positive or negative event-by-event values. Consequently, smaller mean values are obtained, especially in the most central collisions. Fig. 2 shows that the relatively large ground state deformation for ^{158}Dy (open symbols) leads to an increase of $\frac{\varepsilon_4}{(\varepsilon_2)^2}$ [relative to that for the spherical ^{148}Dy isotope] which is especially pronounced in the most central collisions. However, Fig. 3(a) shows that the modest deformation for the Au nuclei does not lead to a similarly increasing trend for $N_{\text{part}} \gtrsim 200$ as implied by data [21, 35].

The relatively flat N_{part} dependence for $\frac{v_4}{(v_2)^2}$, over the range $40 \lesssim N_{\text{part}} \lesssim 200$ in Fig. 3(a), suggests fKLN-like collision geometries. Consequently, it is interesting to investigate whether or not the magnitude of the ratios for $N_{\text{part}} \gtrsim 200$, can be influenced without significant impact on the values for $N_{\text{part}} \lesssim 200$. Figure 3(b) shows that a large increase of $\frac{\varepsilon_4}{(\varepsilon_2)^2}$ can indeed be obtained for $N_{\text{part}} \gtrsim 200$ with relatively little change in the magnitude and trend of the ratios for $N_{\text{part}} \lesssim 200$. This was achieved by introducing a correlation or mixing (m) between the principal axes of the quadrupole (Ψ_2^*) and hexadecapole (Ψ_4^*) density profiles associated with ε_2 and ε_4 respectively. That is, the orientation of Ψ_2^* was modified to obtain the new value $\Psi_2^{**} = (1 - \gamma)\Psi_2^* + \gamma\Psi_4^*$, where $\gamma = 0.2$. This procedure is motivated by the finding that, in addition to the v_4 contributions which stem from the initial hexadecapole density profile, experimental measurements could also have a contribution from v_2 [with magnitude $\propto (v_2)^2$] [29, 37]. The correlation has little, if any, influence on the ε_2 values, but does have a strong influence on $\frac{\varepsilon_4}{(\varepsilon_2)^2}$ in the most central collisions. This is demonstrated in Fig. 3(c) where the double ratio $\frac{R(m)}{R}$ ($R(m) = \frac{\varepsilon_4(m)}{(\varepsilon_2(m))^2}$ and $R = \frac{\varepsilon_4}{(\varepsilon_2)^2}$) is shown.

In summary, we have presented results for the initial eccentricities $\varepsilon_{2,4}$ for collisions of near-spherical and deformed nuclei, for the two primary models currently employed for eccentricity estimates at RHIC. The calculated ratios for $\frac{\varepsilon_4}{(\varepsilon_2)^2}$, which are expected to influence the measured values of $\frac{v_4}{(v_2)^2}$, indicate sizable model dependent differences [both in magnitude and trend] which can be exploited to differentiate between the models. The $\frac{\varepsilon_4}{(\varepsilon_2)^2}$ ratios obtained as a function of N_{part} for Au+Au collisions with the fKLN model ansatz, show trends which are strongly suggestive of the measured ratios for $\frac{v_4}{(v_2)^2}$ observed in Au+Au collisions for $40 \lesssim N_{\text{part}} \lesssim 200$. For more central collisions ($N_{\text{part}} \gtrsim 200$), the observed trend is strongly influenced by initial eccentricity fluctuations if a correlation between the principal axes of the quadrupole and hexadecapole density profiles is assumed. New measurements of $\frac{v_4}{(v_2)^2}$ for collisions of near-spherical and deformed isotopes (or isobars) are required to exploit these tests.

* E-mail: Roy.Lacey@Stonybrook.edu

[1] M. Gyulassy and L. McLerran, Nucl. Phys., **A750**, 30 (2005).

[2] P. Huovinen, P. F. Kolb, U. W. Heinz, P. V. Ruuskanen, and S. A. Voloshin, Phys. Lett., **B503**, 58 (2001).

[3] D. Teaney, Phys. Rev., **C68**, 034913 (2003).

[4] P. Romatschke and U. Romatschke, Phys. Rev. Lett., **99**, 172301 (2007).

[5] Y. Hama *et al.*, Phys. Atom. Nucl., **71**, 1558 (2008).

[6] H. Song and U. W. Heinz, Phys. Rev., **C77**, 064901 (2008).

[7] R. A. Lacey, Nucl. Phys., **A698**, 559 (2002).

[8] R. J. M. Snellings, Nucl. Phys., **A698**, 193 (2002).

[9] J. Adams *et al.*, Phys. Rev. Lett., **92**, 062301 (2004).

[10] R. A. Lacey, A. Taranenko, and R. Wei, (2009), arXiv:0905.4368 [nucl-ex].

[11] U. W. Heinz and S. M. H. Wong, Phys. Rev., **C66**, 014907 (2002).

[12] R. A. Lacey and A. Taranenko, PoS, **CFRNC2006**, 021 (2006).

[13] H.-J. Drescher, A. Dumitru, C. Gombeaud, and J.-Y. Ollitrault, Phys. Rev., **C76**, 024905 (2007).

[14] Z. Xu, C. Greiner, and H. Stocker, Phys. Rev. Lett., **101**, 082302 (2008).

[15] V. Greco, M. Colonna, M. Di Toro, and G. Ferini, (2008), arXiv:0811.3170 [hep-ph].

[16] M. Luzum and P. Romatschke, Phys. Rev., **C78**, 034915 (2008).

[17] A. K. Chaudhuri, (2009), arXiv:0910.0979 [nucl-th].

[18] H. Song and U. W. Heinz, J. Phys., **G36**, 064033 (2009).

[19] T. Hirano, U. W. Heinz, D. Kharzeev, R. Lacey, and Y. Nara, Phys. Lett., **B636**, 299 (2006).

[20] H.-J. Drescher, A. Dumitru, A. Hayashigaki, and Y. Nara, Phys. Rev., **C74**, 044905 (2006).

[21] C. Gombeaud and J.-Y. Ollitrault, (2009), arXiv:0907.4664 [nucl-th].

[22] B. Alver *et al.*, Phys. Rev. Lett., **98**, 242302 (2007).

[23] T. Hirano and Y. Nara, Phys. Rev., **C79**, 064904 (2009).

[24] M. L. Miller, K. Reygers, S. J. Sanders, and P. Steinberg, Ann. Rev. Nucl. Part. Sci., **57**, 205 (2007).

[25] T. Lappi and R. Venugopalan, Phys. Rev., **C74**, 054905 (2006).

[26] H.-J. Drescher and Y. Nara, Phys. Rev., **C76**, 041903 (2007).

[27] S. Raman and C. W. Nestor, Jr., Atom. Data Nucl. Data Tabl., **42**, 1 (1989).

[28] P. Moller, J. R. Nix, W. D. Myers, and W. J. Swiatecki, Atom. Data Nucl. Data Tabl., **59**, 185 (1995).

[29] W. Broniowski, P. Bozek, and M. Rybczynski, Phys. Rev., **C76**, 054905 (2007).

[30] B. B. Back *et al.* (PHOBOS), Phys. Rev., **C70**, 021902

(2004).

[31] E. V. Shuryak, Phys. Rev., **C61**, 034905 (2000).

[32] B.-A. Li, Phys. Rev., **C61**, 021903 (2000).

[33] U. W. Heinz and A. Kuhlman, Phys. Rev. Lett., **94**, 132301 (2005).

[34] P. Filip, R. Lednicky, H. Masui, and N. Xu, Phys. Rev.,

C80, 054903 (2009).

[35] and A. Adare (The PHENIX), (2010), arXiv:1003.5586 [nucl-ex].

[36] U. W. Heinz, J. S. Moreland, and H. Song, Phys. Rev., **C80**, 061901 (2009).

[37] P. F. Kolb, L.-W. Chen, V. Greco, and C. M. Ko, Phys. Rev., **C69**, 051901 (2004).